

Electronic Supplementary Information

Water-stable Lanthanide-based Metal–Organic Gel for Detection of Organic Amines and White-Light Emission

Dongxu Gu,^a Weiting Yang,^{*a} Duoyu Lin,^a Xudong Qin,^a Yonghang Yang,^a Fuxiang Wang,^a Qinhe Pan,^{*a} Zhongmin Su^{*b}

^a *Key laboratory of Advanced Materials of Tropical Island Resources, Ministry of Education, School of Science, Hainan University, Haikou, 570228, P. R. China.*

^b *Jilin Provincial Science and Technology Innovation Center of Optical Materials and Chemistry, School of Chemistry and Environmental Engineering, Changchun University of Science and Technology, Changchun 130022, P. R. China.*

Email: yangwt@hainanu.edu.cn; panqinhe@163.com; zmsu@nenu.edu.cn

Contents

Experimental	3
Materials and methods	3
Synthesis of Ln-MOG	3
Synthesis of Tb-MOG testing paper	3
Fluorescence measurement	4
Table S1. Synthesis optimized scheme of Tb-MOG	5
Table S2. Synthesis scheme of Ln-MOG with different Tb ³⁺ /Eu ³⁺ ratio	6
Table S3. EDS analysis of Ln-MOG	7
Table S4. Fitting parameters and detection limits of Tb-MOG for organic amines in water.	8
Table S5. Fitting parameters and detection limits of Tb-MOG for organic amine vapors.	9
Fig. S1 Structure of 3,5-di(2',4'-dicarboxylphenyl)benzoic acid (DPBA) and images of the Tb-MOG	10
Fig. S2 EDS-Mapping of Ln-MOG	11
Fig. S3 PXRD pattern of Tb-MOG before and after immersed in TEA aqueous solution	12
Fig. S4 Fourier transform infrared (FTIR) spectra of DPBA and Tb-MOG	13
Fig. S5 Pictures of synthetic gel under different conditions	14
Fig. S6 Change of fluorescence intensity of Tb-MOG aqueous dispersion with time	15
Fig. S7 Fluorescence spectra of Tb-MOG after adding different organic molecules	16
Fig. S8 Optical photo of Tb-MOG testing paper under UV lamp irradiation.	17
Fig. S9 Schematic of organic amine vapor detection device	18
Fig. S10 Fluorescence spectra of Tb-MOG testing paper recorded under different concentrations of organic amine vapor.	19
Fig. S11 SEM image of Tb-MOG after immersed in TEA aqueous solution	20
Fig. S12 Emission spectra of Tb-MOG under different excitations.	21
Fig. S13 Excitation and emission spectra of Eu-MOG	22
Fig. S14 Emission spectrum of Tb _{0.92} Eu _{0.08} -MOG.	23
Fig. S15 CIE coordinates of Tb/Eu-MOG under different excitations	24
Notes and references	25

Experimental

Materials and methods

The morphology was recorded by Phenom ProX desktop scanning electron microscopy (Phenom-World, Netherlands). Powder X-ray diffraction (PXRD) data were obtained by Rigaku Miniflex 600 X-Ray Diffractometer with Cu K α ($\lambda = 1.5418 \text{ \AA}$) radiation at 40 kV and 15 mA. Fluorescence spectra were collected on a GangDong F-320 fluorescence spectrophotometer at room temperature. X-ray photoelectron spectroscopy (XPS) measurements were performed in a stainless-steel ultrahigh vacuum chamber (Thermo Fisher, Escalab250xi, base pressure $< 10^{-10}$ mbar). The inductively coupled plasma mass spectrometry (ICP) results were tested by the Agilent ICPOES 730 instrument. Fourier transform infrared (FTIR) spectra were acquired with KBr disks in the range of 4000–400 cm^{-1} on a Nicolet 6700 IR spectrometer. UV-vis spectra were measured on UV spectrophotometer (UV-2700, Shimadzu instruments (Suzhou) Co., Ltd.). The quantum yield was measured on the FLS980 steady-state/cis-state fluorescence spectrometer (Edinburgh instruments). The DPBA ligand was purchased from Jinan Henghua Sci. & Tec. Co., Ltd (Jinan China), and the structure of DPBA is shown in Fig. S1. Other reagents and solvents were purchased from commercial sources and used without further purification.

Synthesis of Tb-MOG

0.05 mmol of $\text{Tb}(\text{NO}_3)_3 \cdot 6\text{H}_2\text{O}$ and 0.05 mmol of DPBA was mixed in 2.5 mL DMF and 0.5 mL H_2O . Then the resulting solution was sealed in 10 mL glass vial and heated at 95°C for 24 h, resulting in a white Tb-MOG. The homogenous Tb-MOG and dried under 85°C for 36 h to obtain xerogel. After filtration and being washed with DMF for several times, white xerogel of Tb-MOG was collected. The synthetic conditions showing different ratios of $\text{H}_2\text{O}/\text{DMF}$ and $\text{Tb}^{3+}/\text{DPBA}$ are shown in Table S1, and the images of corresponding products are displayed in Fig. S5. During the optimization of Tb-MOGs, the composition of solvents and reactants is important for the gel formation. First, the amount of water is crucial in that when the proportion of $\text{H}_2\text{O}/\text{DMF}$ was lower than 1/5, the reaction cannot produce a gel but a clear solution (MOG-1). While when the proportion was higher than 1/5, the occurrence of precipitate was observed (MOG-3-5). Gel materials were formed in a normal manner under $\text{H}_2\text{O}/\text{DMF}$ proportion of 1/5

(MOG-2), which may be related to the construction of the hydrogen bond network in presence of water. However, too much water will reduce the solubility of DPBA, which is not conducive to gel formation. Second, the proper concentrate of Tb^{3+} is necessary. When the content of Tb^{3+} was lower than 0.05 mmol in 3 mL of DMF/ H_2O , the gel was unable formed (MOG-6-7). Higher concentration will lead to colloidal with weak mechanical strength (MOG-9-10). Last, Tb-MOGs can be formed normally when the molar ratio of Tb^{3+} and DPBA ligand is close to 1/1 (MOG-8). On the Other hand, a certain range of reaction temperature (70-120 °C) and time (> 20 h) is effective for the formation of gel products.

Synthesis of Eu-MOG

Eu-MOG was prepared by similar methodology using 0.1 mmol of $Eu(NO_3)_3 \cdot 6H_2O$ instead of $Tb(NO_3)_3 \cdot 6H_2O$. To synthesize Tb/Eu-MOG, different proportions of Tb^{3+} , Eu^{3+} and 0.5 mL solution of DPBA (0.1 M in DMF) were mixed in 2 mL of DMF (Table S2†). The xerogels were obtained in the similar way as the xerogel of Tb-MOG.

Synthesis of Tb-MOG testing paper

0.1 g of Tb-MOG xerogel was dispersed in 5 mL of water and stirred at room temperature for 1 h to form Tb-MOG dispersion. A commercial filter paper with a diameter of 7 cm is fixed on Glue machine (speed = 1000 rpm, t = 180 s, acceleration = 800 rpm/s). 3 mL of the dispersion was dropped on the filter paper, and then the filter paper was removed and dried at 60 °C to prepare the Tb-MOG testing paper.

Fluorescence measurement

To detect organic amines in solution, the xerogel of Tb-MOG (3 mg) was immersed in 15 mL of aqueous solutions with different concentrations of EDA, TEA, DIPA and AN at room temperature. The fluorescence spectra were collected after sonication for 30 s.

The experiments of organic amine vapor detection were carried out in the device shown in Fig. S9. The sensing device was placed under ambient condition (22 °C with the relative humidity of 65%). The concentration of organic amine vapor was calculated according to the following equation:¹

$$C = \frac{22.4\rho TV_s \times 10^3}{273MV} \quad (1)$$

where C is the concentration of organic amine (ppm), ρ is the density of liquid organic amine (g mL^{-1}), T is the temperature of testing chamber (K), V_s is the volume of liquid organic amine (μL), M is the molecular weight of organic amine (g mol^{-1}), and V is the volume of the chamber (L). In our work, the parameters are as follows: TEA ($M = 101 \text{ g mol}^{-1}$, $\rho = 0.728 \text{ g mL}^{-1}$), EDA ($M = 60 \text{ g mol}^{-1}$, $\rho = 0.90 \text{ g mL}^{-1}$) and DIPA ($M = 101 \text{ g mol}^{-1}$, $\rho = 0.718 \text{ g mL}^{-1}$) and T (295 K).

Table S1. Synthesis optimized scheme of Tb-MOG with different DMF/H₂O and Tb³⁺/DPBA ratio (T = 95 °C, t = 24 h).

Tb(NO ₃) ₃ ·6H ₂ O (mmol)	DPBA (mmol)	H ₂ O (mL)	DMF (mL)	Named
0.05	0.05	0	3	MOG-1
0.05	0.05	0.5	2.5	MOG-2
0.05	0.05	1	2	MOG-3
0.05	0.05	1.5	1.5	MOG-4
0.05	0.05	2	1	MOG-5
0.01	0.05	0.5	2.5	MOG-6
0.03	0.05	0.5	2.5	MOG-7
0.05	0.05	0.5	2.5	MOG-8
0.07	0.05	0.5	2.5	MOG-9
0.09	0.05	0.5	2.5	MOG-10

Table S2. Synthesis scheme of Ln-MOG with different Tb³⁺/Eu³⁺ ratio. The concentration of Ln(NO₃)₃•6H₂O aqueous solution is 0.1 M (Ln = Tb or Eu).

Tb(NO ₃) ₃ •6H ₂ O (μL)	Eu(NO ₃) ₂ •6H ₂ O (μL)	Molar ratio of Tb:Eu
300	200	60:40
340	160	68:32
380	120	76:24
420	80	84:16
460	40	92:8

Table S3. EDS analysis of Ln-MOG. (Count by wt% of the element)

Sample	C	O	N	Tb	Eu	Total
Tb-MOG	41.9	14.3	5.3	38.5	-	100
Eu-MOG	45.2	17.3	4.3	-	33.2	100
Eu/Tb-MOG	47.3	12.3	8.7	27.2	4.5	100

Table S4. Fitting parameters and detection limits of Tb-MOG for organic amines in water.

Amine	y=a+bx			LOD
	a	b	R ²	
EDA	-0.00735±0.008	0.0426±0.0011	0.996	0.23 ppm
TEA	0.0118±0.006	0.0359±0.0009	0.997	0.27 ppm
DIPA	0.0811±0.0043	0.0374±0.0008	0.998	0.26 ppm
AN	-0.0545±0.0093	0.0229±0.0007	0.994	0.43 ppm

Table S5. Fitting parameters and detection limits of Tb-MOG testing paper for organic amine vapors.

Amine	y=a+bx			LOD
	a	b	R ²	
TEA	0.00625±0.00887	0.01019±0.00016	0.996	0.98 ppm
EDA	-0.0848±0.01671	0.00943±0.00027	0.992	1.06 ppm
DIPA	0.07356±0.01024	0.00857±0.00017	0.997	1.17 ppm

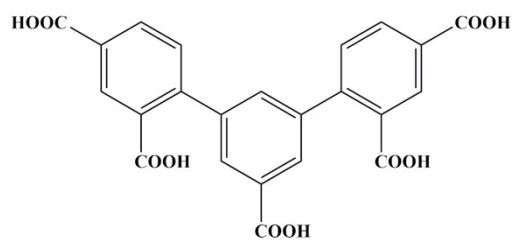


Fig. S1 Structure of 3,5-di(2',4'-dicarboxylphenyl)benzoic acid (DPBA).

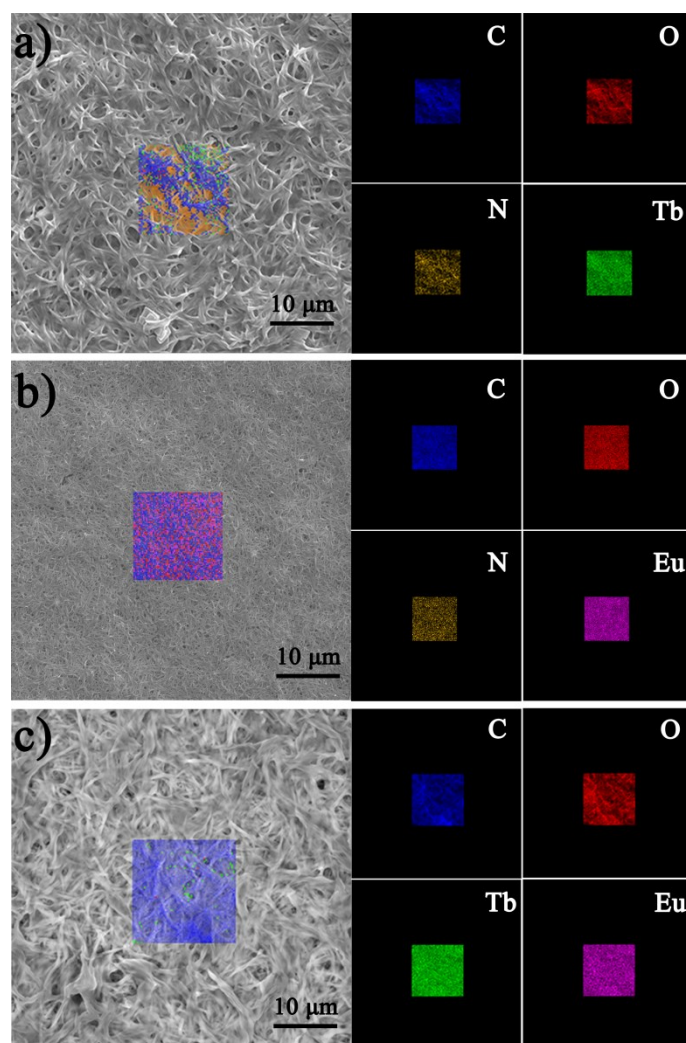


Fig. S2 SEM-Mapping of Tb-MOG (a), Eu-MOG (b) and Tb_{0.84}/Eu_{0.16}-MOG (c).

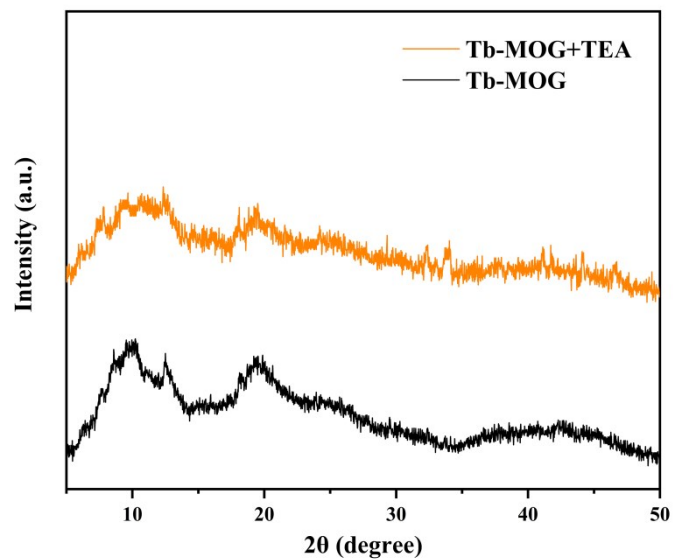


Fig. S3 PXR D pattern of Tb-MOG before and after immersed in TEA aqueous solution (100 ppm) for 6 h.

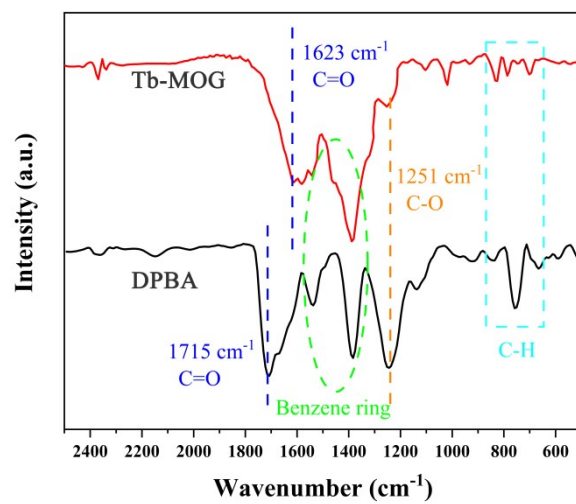


Fig. S4 Fourier transform infrared (FTIR) spectra of DPBA and Tb-MOG.

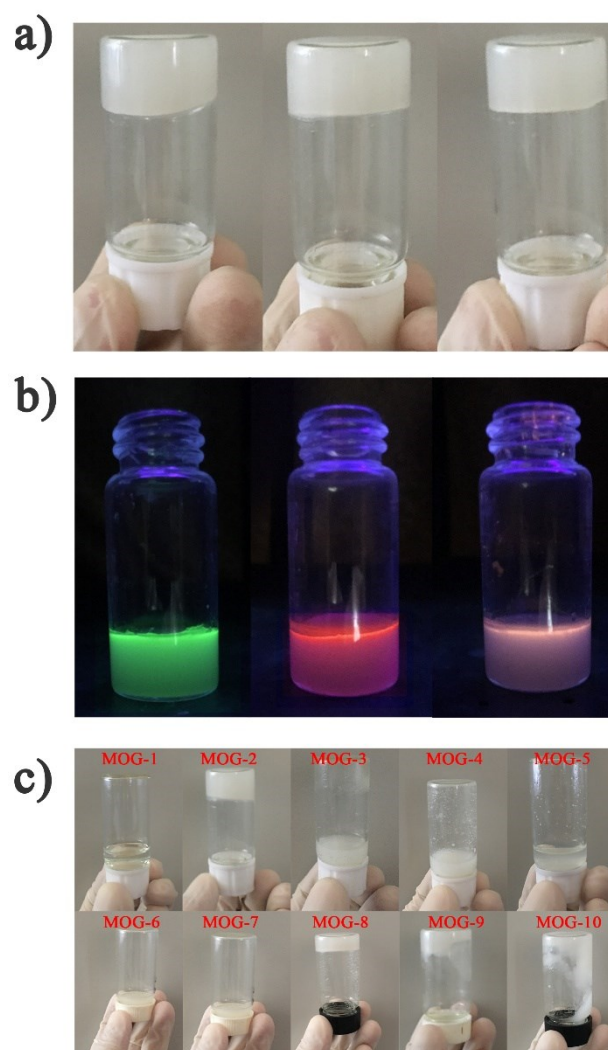


Fig. S5 Photos of Ln-MOG under natural light (a) and UV irradiation (b, 254 nm). Left: Tb-MOG, middle: Eu-MOG, right: Tb_{0.84}Eu_{0.16}-MOG. (c) The pictures of synthetic gel under different conditions

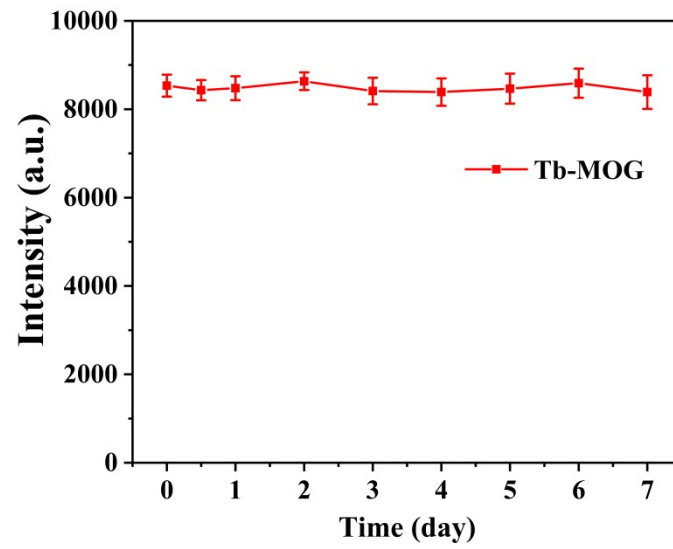


Fig. S6 Change of fluorescence intensity of Tb-MOG aqueous dispersion with time (monitored at 544 nm).

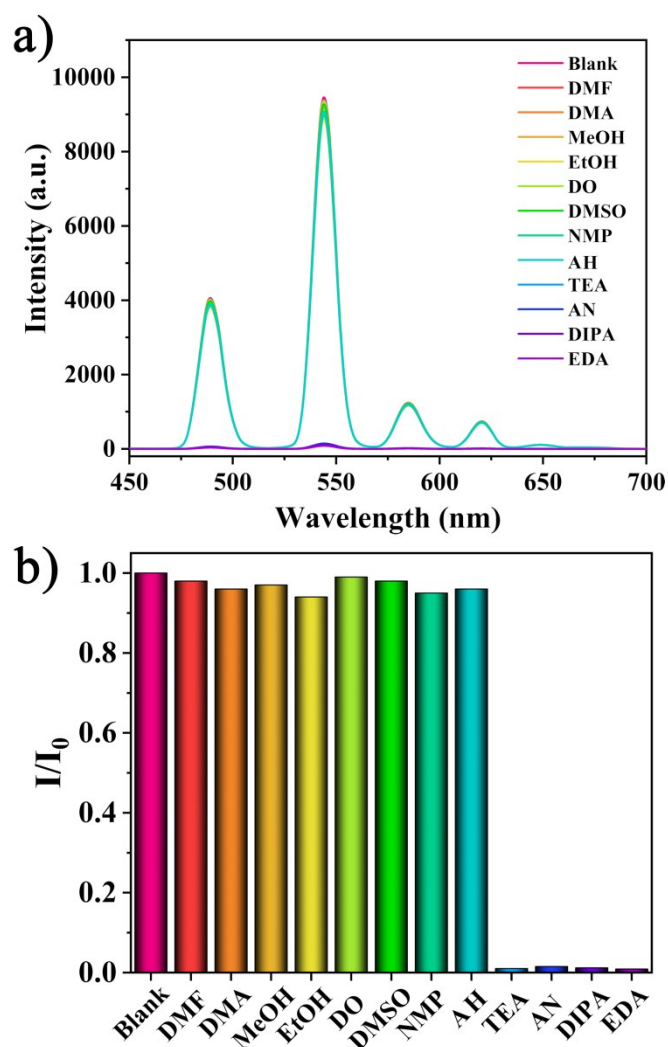


Fig. S7 (a) Fluorescence emission spectra of Tb-MOG dispersed in aqueous solutions with various organic molecules (200 ppm) including DMF, DMA, MeOH, EtOH, 1,4-dioxane (DO), Dimethyl sulfoxide (DMSO), N-Methyl pyrrolidone (NMP), ammonium hydroxide (AH), TEA, EDA, DIPA and AN. (b) Relative fluorescence intensity of Tb-MOG after adding various analytes monitor at 544 nm.

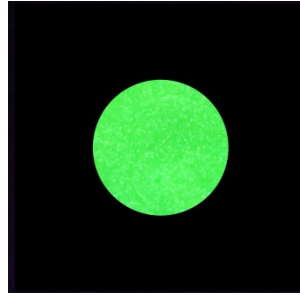


Fig. S8 Optical photo of Tb-MOG testing paper under UV lamp irradiation (254 nm).

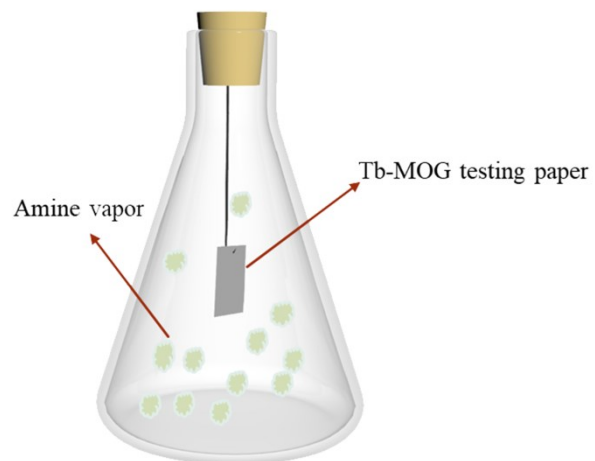


Fig. S9 Schematic of organic amine vapor detection device

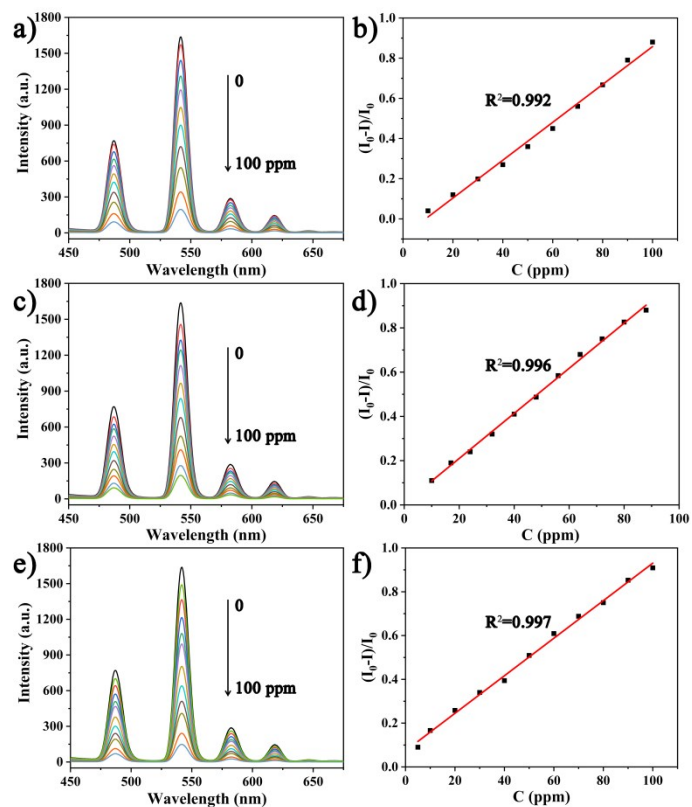


Fig. S10 Fluorescence spectra of Tb-MOG testing paper recorded under increasing the concentration vapors of EDA (a) TEA (c) DIPA (e). The data points are fitted in a linear relationship under different EDA (b) TEA (d) and DIPA (f) vapor concentrations (measured at 544 nm).

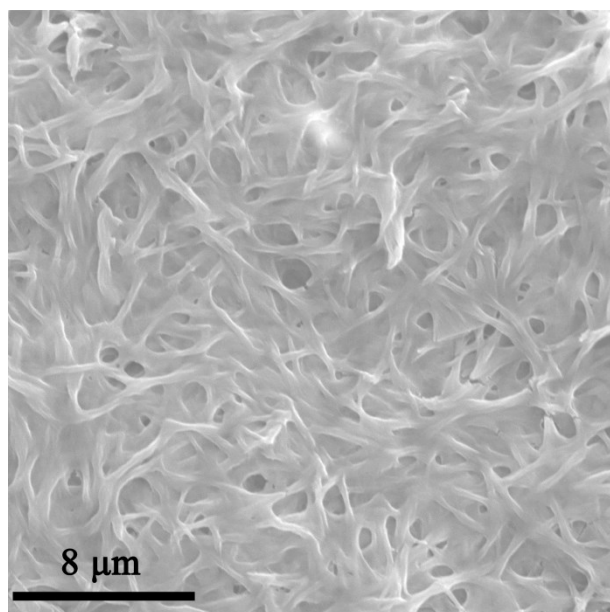


Fig. S11 SEM image of Tb-MOG after immersed in TEA aqueous solution (100 ppm) for 6 h.

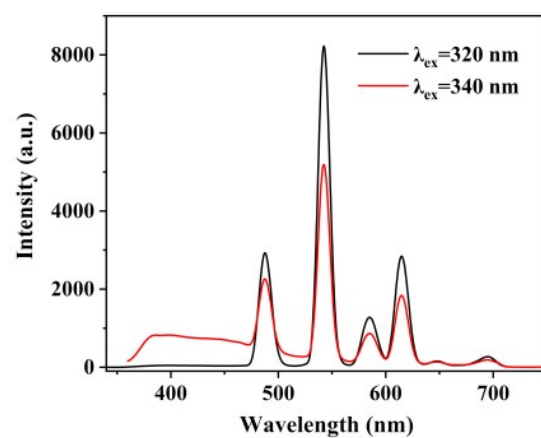


Fig. S12 Emission spectra of Tb-MOG under different excitations.

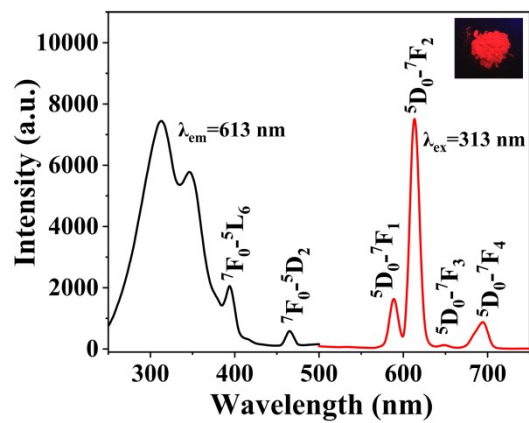


Fig. S13 Excitation and emission spectra of Eu-MOG. Insert: the image of Eu-MOG under UV lamp irradiation (254 nm).

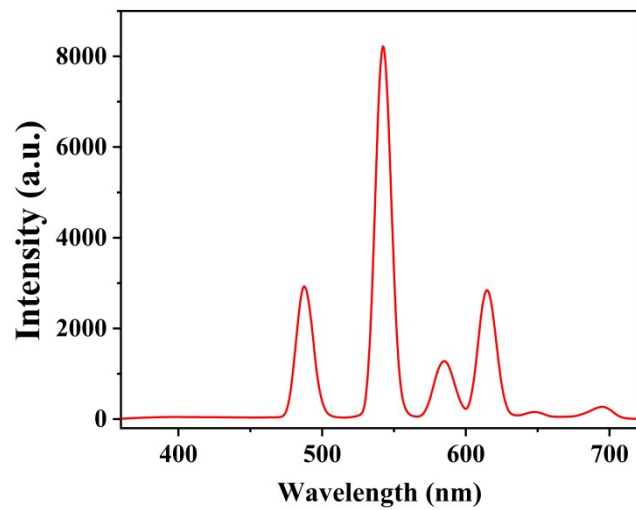


Fig. S14 Emission spectrum of Tb_{0.92}Eu_{0.08}-MOG ($\lambda_{\text{ex}} = 320$ nm).

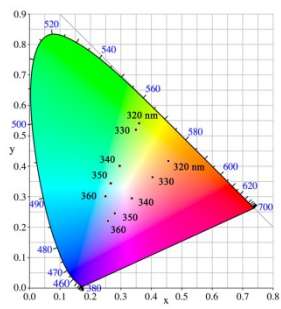


Fig. S15 CIE coordinates of Tb_x/Eu_{1-x} -MOG ($x=0.92, 0.76$) under different excitations.

Notes and references

- 1 X. Wang, F. Cui, J. Lin, B. Ding, J. Yu and S. Al-Deyab, *Sens. Actuators B*, 2012, **171-172**, 658-665.